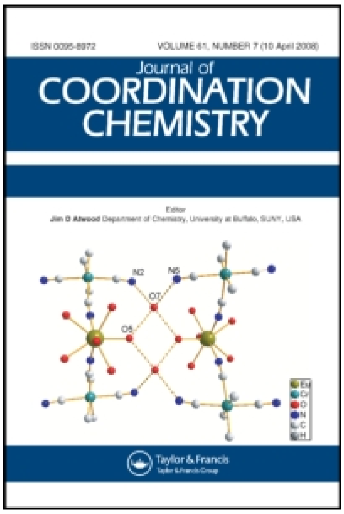

Journal of Coordination Chemistry
Publication details, including instructions for authors and subscription information:
http://www.informaworld.com/smpp/title~content=t713455674

Synthesis, characterization and SOD-like activity of a ternary copper(II) complex with 1,10-phenanthroline and L-arginine

Hui Fang Ma[a]; Xi Rui Zeng[b]; Xiao Hua Zhou[a]; Shi Chen[a]; Chun Lin Ni[a]
[a] Department of Applied Chemistry, College of Science, South China Agricultural University, Guangzhou 510642, P.R. China [b] Provincial Key Laboratory of Coordination Chemistry, Chemistry & Chemical Engineering College, Jinggangshan College, Ji'an 343009, P.R. China

To cite this Article Fang Ma, Hui , Rui Zeng, Xi , Hua Zhou, Xiao , Chen, Shi and Lin Ni, Chun(2008) 'Synthesis, characterization and SOD-like activity of a ternary copper(II) complex with 1,10-phenanthroline and L-arginine', Journal of Coordination Chemistry, 61: 23, 3829 — 3838

To link to this Article: DOI: 10.1080/00958970802150090

URL: http://dx.doi.org/10.1080/00958970802150090

Journal of Coordination Chemistry
Vol. 61, No. 23, 10 December 2008, 3829–3838

Taylor & Francis
Taylor & Francis Group

Synthesis, characterization and SOD-like activity of a ternary copper(II) complex with 1,10-phenanthroline and L-arginine

HUI FANG MA†, XI RUI ZENG‡, XIAO HUA ZHOU*†, SHI CHEN†
and CHUN LIN NI†

†Department of Applied Chemistry, College of Science, South China Agricultural
University, Guangzhou 510642, P.R. China
‡Provincial Key Laboratory of Coordination Chemistry, Chemistry & Chemical Engineering
College, Jinggangshan College, Ji'an 343009, P.R. China

(*Received 14 July 2007; in final form 21 September 2007*)

The new complex $[Cu(phen)(L\text{-arg})Cl]_2 \cdot 7H_2O$ was prepared and characterized by elemental analysis, molar conductivity, IR, UV–Vis and X-ray diffraction methods. It crystallizes in the triclinic space group $P\bar{1}$ with four molecules in a unit cell of dimensions, $a = 10.3733(13)$ Å, $b = 12.4269(15)$ Å, $c = 18.926(2)$ Å, $\alpha = 94.627(2)^\circ$, $\beta = 104.864(2)^\circ$, $\gamma = 101.032(2)^\circ$, $V = 2292.8(5)$ Å^3, $Z = 2$, $D_c = 1.493\,\mathrm{g\,cm^{-3}}$, $\mu = 1.004\,\mathrm{mm^{-1}}$, $F(000) = 1072$, $R_{\mathrm{int}} = 1.113$ for 7290 unique reflections. The superoxide dismutase-like activity of the complex for catalyzing the dismutation of $O_2^{\cdot -}$ was determined by the NBT method. The complex has high superoxide dismutase-like activity and the rate constant (K_Q) of complex for catalyzing the dismutation of $O_2^{\cdot -}$ is $5.19 \times 10^7\,\mathrm{mol^{-1}\,dm^3\,s^{-1}}$. CCDC: 645352

Keywords: Copper (II); 1,10-Phenanthroline; *L*-arginine; Crystal structure; Superoxide dismutase(SOD); SOD-like activity

1. Introduction

Superoxide anion ($O_2^{\cdot -}$) is essential as a defense system against the invasion of bacteria and viruses and serves important roles as a signaling molecule and even as a terminator of lipid peroxidation [1]. $O_2^{\cdot -}$ is increasingly known to be associated tightly with the pathogenesis of many diseases [2]; especially when organisms were under stress such as toxicant, irradiation, hypoxia, freezing, drought, etc., $O_2^{\cdot -}$ would overproduce and become poisonous and surplus $O_2^{\cdot -}$ would initiate lipid peroxidation [3], cause nucleic acid and protein damage [4–6] and influence cellular signaling [7]. Thus humans would undergo neurondegenerative diseases [8, 9], aging [10] even cancer [11, 12] and plants might grow slowly [13, 14] or die. Luckily, in humans, animals and plants there are native metal enzymes, superoxide dismutases (SOD), which change the dismutation of $O_2^{\cdot -}$ into H_2O_2 and O_2. Applications in clinical medicine of native SODs have been in a dilemma because of huge molecular weight, high costs and the major problem of oxidant–antioxidant balance [2]. To make up for such limitations with hope for

---

*Corresponding author. Email: zhouxiaohua1970@163.com

Journal of Coordination Chemistry
ISSN 0095-8972 print/ISSN 1029-0389 online © 2008 Taylor & Francis
DOI: 10.1080/00958970802150090

widespread clinical use based on superoxide-scavenging mechanisms, research has focused on synthesizing CuZn–SOD mimics that have low molecular weight, low-toxicity [15] and cost-effectiveness.

Zn(II) plays a predominant structural role in native CuZn–SOD. The Cu(II) ion, on the other hand, is the true active center, binding superoxide [16]. So copper(II) complexes with the same coordination sphere as the Cu-bonding site in CuZn–SOD, in which the Cu^{2+} is coordinated to four imidazole nitrogen atoms and an axial water, forming a distorted square-pyramidal geometry, can be used as CuZn–SOD mimics. [17–21] Several ternary copper-amino acid complexes, which possess distorted square-pyramidal geometry, have been reported as SOD mimics [22, 23]. In this study a new SOD mimic $[Cu(phen)(L\text{-arg})Cl]_2 \cdot 7H_2O$ has been synthesized and characterized by elemental analysis, molar conductivity, IR spectra and UV–Vis spectra and X-ray diffraction methods. The catalytic activity of the complex for dismutation of $O_2^{\cdot -}$ was determined by the NBT method. The results show that the complex has distinct SOD-like activities in water.

2. Experimental

2.1. *Synthesis*

The complex was prepared by reaction of CuCl (0.05 g, 0.5 mmol) in 0.25 mL condensed hydrochloric acid and 1,10-phenanthroline monohydrate (0.1 g, 0.5 mmol) in 6 mL of anhydrous ethanol, followed by addition of 10 mL of aqueous solution of *L*-arginine (0.09 g, 0.6 mmol), and adjusting the pH to 5 ~ 6 with aqueous NaOH solution. The solution was stirred and heated for 30 min, then cooled and filtered. The resulting solution was left to evaporate at room temperature. Blue crystals of the desired complex formed after three weeks, were filtered and air-dried (82%yield). Anal. Calcd for $C_{36}H_{56}Cl_2Cu_2N_{12}O_{11}$ (%): C, 41.91; H, 5.43; N, 16.30. Found: C, 42.03; H, 5.13; N, 16.74. Molar conductivity: $35.2\,S\,cm^{-2}\,mol^{-1}$.

2.2. *Physical measurements*

The elemental analysis (carbon, nitrogen and hydrogen) was performed on a Perkin-Elmer 240 microanalyzer. The infrared absorption spectra in KBr discs were recorded in the 400–4000 cm^{-1} range at room temperature on a Nicolet 170SX spectrophotometer. The electronic absorption spectrum of the complex was measured in water on a Pharmacia 4000 UV–Vis spectrophotometer at room temperature. Molar conductivities were carried out in ethanol using a DDS-11A.

2.3. *X-ray structural determination*

A single crystal ($0.28 \times 0.30 \times 0.42\,mm^3$) of the complex was selected for X-ray diffraction measurement on a Bruker Smart 1K CCD system diffractometer with graphite monochromatic Mo-Kα radiation at $\lambda = 0.71073$ Å. The SMART program was applied to search for diffraction peaks to determine cell parameters, and the collected data were reduced using the SAINT+ program [24]. Absorption corrections were applied with the Siemens Area Detector Absorption (SADABS) program [25].

The structure was solved by direct and Fourier methods, and refinements were carried by full-matrix least squares on F^2 with positional and anisotropic thermal parameters. The atomic coordinates anisotropic thermal parameters for non-hydrogen atoms were refined to converge. All hydrogen atoms were placed in calculated positions. Atomic scattering factors were taken from International Tables for *X*-ray Crystallography [26]. All calculations were performed on a PC with the Siemens SHELXS-97 [27] and SHELXL-97 [28] program packages. The crystal data and refinement parameters are summarized in table 1.

2.4. *Measurement of SOD activity*

SOD-like activity of the complex was determined by the modified nitroblue tetrazolium (NBT) photo reduction [29]. Mixed solution containing NBT (9.32×10^{-5} M), riboflavin (6.80×10^{-6} M), and tetramethyl ethylenediamine (1.0×10^{-4} M) in phosphate buffer at pH 7.8 was used as blank solution, and solutions containing concentrations of complex ($10^{-6} \sim 10^{-8}$ M) or native CuZn–SOD ($0.005 \sim 0.0\ \mu\text{mol dm}^{-3}$) in the blank solution were considered as competitive solutions. The superoxide anion was generated by illumination under a fluorescence lamp and detected with spectrophotometer by monitoring the formation of the NBT reduction at 560 nm. The NBT reduction rate was measured in the presence and absence of CuZn–SOD or the investigated complex for 210 s. All measurements were carried out at 25 ± 0.2C using 1 cm × 1 cm

Table 1. Crystal data and structure refinement for $[Cu(phen)(L\text{-arg})Cl]_2 \cdot 7H_2O$.

Empirical formula	$C_{36}H_{56}Cl_2Cu_2N_{12}O_{11}$
Formula weight	1030.91
Temperature (K)	273(2)
Wavelength (Å)	0.71073
Crystal system	Triclinic
Space group	$P\bar{1}$
Unit cells dimensions (Å, °)	
a	10.3733(13)
b	12.4269(15)
c	18.926(2)
α	94.627(2)
β	104.864(2)
γ	101.032(2)
V (Å^3)	2292.8(5)
Z	2
D_{Calcd} (g cm^{-3})	1.493
$F(000)$	1072
R_{int}	1.113
θ range for data collection (°)	$1.89 \sim 26.10$
Limiting indices	$-12 \le h \le 11$, $-15 \le k \le 15$, $-23 \le l \le 23$
Reflections collected/unique	14929/7290
Data/restraints/parameters	8282/23/600
Goodness-of-fit on F^2	1.004
Final R indices [$I > 2\sigma(I)$]	$R_1 = 0.1221$; $wR_2 = 0.4596$
R indices (all data)	$R_1 = 0.1168$; $wR_2 = 0.4443$
Largest diff. peak and hole (e Å^{-3})	4.43 and −0.86

thermostatic cuvettes. The IC_{50} (the concentration of CuZn–SOD or the complex which causes 50% inhibition of NBT reduction) of native CuZn–SOD or the complex was calculated. Each final result for IC_{50} is the average of at least three independent determinations, and the relative error is less than 1.4%.

To test the influence of small amounts of copper ions, phen and *L*-arg, which are dissociated slightly from the complex, the control experiment was performed with $CuCl_2$, phen and *L*-arg.

3. Results and discussion

Elemental analysis of the title complex is in good agreement with the formula $[Cu(phen)(L\text{-arg})Cl]_2 \cdot 7H_2O$. The complex is soluble in water, methanol and ethanol, but not in ether and other low polarity organic solvents. Molar conductivity measurement in ethanol at $10^{-3}\,mol\,L^{-1}$, $\Lambda_m = 35.2\,S\,cm^2\,mol^{-1}$, show a non-electrolyte [30].

3.1. *Crystal structure*

Figure 1 shows the perspective view of $[Cu(phen)(L\text{-arg})Cl]_2$, and figure 2 shows the crystal packing view of the title complex, in which the hydrogen atoms and crystal waters are omitted for clarity.

Complex consists of neutral $[Cu(phen)(L\text{-arg})Cl]$ and seven crystal water molecules. In the unit cell there are four independent molecules and in each molecule the Cu(II) is in a slightly distorted square-pyramidal geometry, with two nitrogen atoms of 1,10-phenanthroline(N,N), one amino nitrogen atom and one carboxylate oxygen atom of *L*-arginate(N,O) in the equatorial plane ($d(Cu–O) = 1.945 \sim 1.960\,Å$, $d(Cu–N) = 1.982 \sim 2.043\,Å$) and a chloride in the apical position ($d(Cu–Cl) = 2.50 \sim 2.62\,Å$). The bond lengths in the complex are similar to corresponding values found for $[Cu(L\text{-val})(phen)\ (H_2O)] \cdot ClO_4$ (Equatorial plane: $d(Cu–O) = 1.928\,Å$, $d(Cu–N) = 1.991 \sim 2.009\,Å$; axial: $d(Cu–O) = 2.272\,Å$) [31], $[Cu_2(L\text{-arg})_2(bpy)_2\,(\mu_2\text{-}ClO_4)_2] \cdot 2ClO_4 \cdot H_2O\}_n$ (Equatorial plane: $d(Cu–O) = 1.922 \sim 1.929\,Å$, $d(Cu–N) = 1.989 \sim 2.009\,Å$;

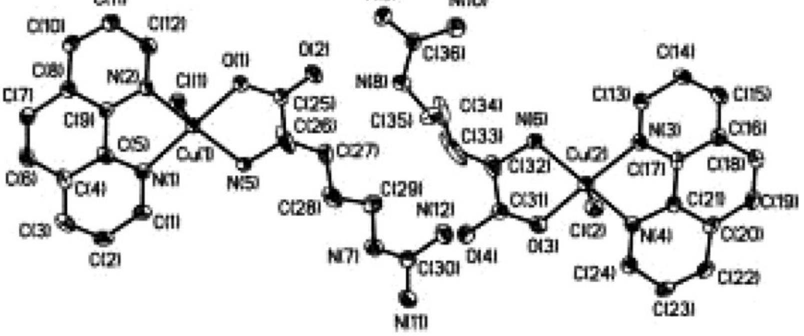

Figure 1. ORTEP plot showing the structure of $[Cu(phen)(L\text{-arg})Cl]_2$, and the atom-numbering scheme.

axial: d(Cu–O) = 2.503 ~ 2.593 Å) [32]. The square-pyramidal geometry around Cu(II) is severely distorted, with X–Cu–Z angles being 163.0° to 169.9° where X and Z are any two atoms in para positions and the X–Cu–Y angles ranging from 81.9° to 101.1° where X and Y are any two atoms ortho. Selected bond lengths and angles are given in table 2. N1, N2, O1, N5 and Cu1 atoms deviate by 0.3135, 0.6655, 1.0535, 0.3371 and 0.6266 Å, and N3, N4, O3, N6 and Cu2 atoms deviate by 0.4213, −0.3988, −0.6652, 0.2337 and −0.3183 Å, respectively, from the least-squares plane ($-4.5596x - 3.3863y - 16.9224$

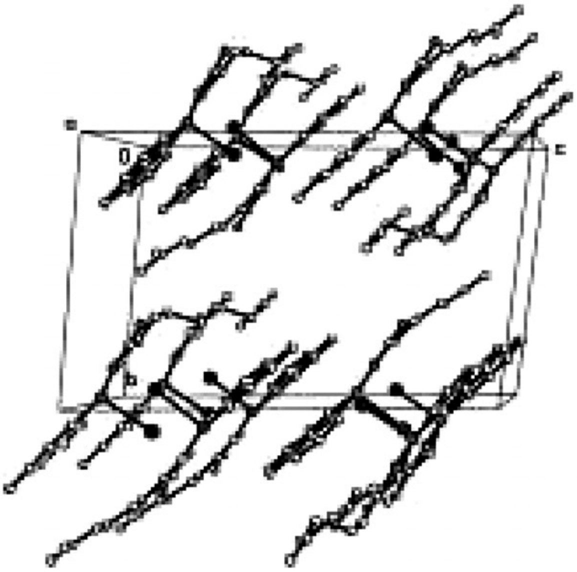

Figure 2. Crystal packing view for complex $[Cu(phen)(L\text{-}arg)Cl]_2 \cdot 7H_2O$, in which the crystal waters and hydrogen atoms are omitted for clarity.

Table 2. Selected bond lengths (Å) and angles (°) of $[Cu(phen)(L\text{-}arg)Cl]_2 \cdot 7H_2O$.

Cu(1)–O(1)	1.960(5)	Cu(2)–O(3)	1.945(5)
Cu(1)–N(5)	1.982(6)	Cu(2)–N(4)	2.014(7)
Cu(1)–N(2)	2.000(6)	Cu(2)–N(6)	2.033(6)
Cu(1)–N(1)	2.029(6)	Cu(2)–N(3)	2.043(6)
Cu(1)–Cl(1)	2.6208(19)	Cu(2)–Cl(2)	2.5049(19)
N(8)–C (36)	1.346(10)	C (36)–N(9)	1.294(11)
C(36)–N(10)	1.359(10)	C(30)–N(7)	1.285(11)
C(30)–N(11)	1.340(10)	C(30)–N(12)	1.324(11)
O(1)–Cu(1)–N(5)	83.9(2)	O(3)–Cu(2)–N(4)	90.4(2)
O(1)–Cu(1)–N(2)	91.7(2)	O(3)–Cu(2)–N(6)	83.9(2)
N(5)–Cu(1)–N(2)	170.5(2)	N(4)–Cu(2)–N(6)	164.1(3)
O(1)–Cu(1)–N(1)	163.3(3)	O(3)–Cu(2)–N(3)	166.2(2)
N(5)–Cu(1)–N(1)	99.9(2)	N(4)–Cu(2)–N(3)	81.9(3)
N(2)–Cu(1)–N(1)	81.9(3)	N(6)–Cu(2)–N(3)	100.4(3)
O(1)–Cu(1)–Cl(1)	100.88(17)	O(3)–Cu(2)–Cl(2)	99.48(18)
N(5)–Cu(1)–Cl(1)	92.61(19)	N(4)–Cu(2)–Cl(2)	99.01(17)
N(2)–Cu(1)–Cl(1)	96.51(18)	N(6)–Cu(2)–Cl(2)	96.5(2)
N(1)–Cu(1)–Cl(1)	95.17(19)	N(3)–Cu(2)–Cl(2)	93.07(17)

$z = -6.0307$), showing that the five ligating atoms in the coordination sphere are approximately coplanar. The nitrogens of *L*-arginate guanidine are not coordinated to the central copper and the bond lengths and angles of the guanidine C–N bonds are analogous to literature [32]. Thus many intermolecular H-bonds [N $\cdots$ O $= 2.855 \sim 3.076$ Å(moderate strength), N $\cdots$ Cl $=$ $3.219 \sim 3.358$ Å (weak strength)] are formed among the guanidine nitrogens, seven crystal water oxygens and uncoordinated carboxylate oxygen of *L*-arginate. In addition, the average distance between intermolecular phen-rings is 3.586 Å, indicating intermolecular phen-ring stacking interactions in the crystal. Figure 3 shows the intermolecular aromatic-stacking interaction. Intermolecular aromatic-stacking and hydrogen-bond interactions make the single crystal exhibit the -a-b-a-b- type crystal structure similar to that observed in [Cu(phen)(*L*-val)(H_2O)]Cl $\cdot$ H_2O [19], [Cu(H_2O) (*L*-met)(phen)]$ClO_4 \cdot 2H_2O$ [33] and [Cu(L-val)(phen) (H_2O)] $\cdot$ ClO_4 [31]. Selected intermolecular H-bonds are shown in table 3.

The oxidation state of central copper in the complex is II although the reactant material is cuprous chloride, explained by the instability of cuprous in water.

3.2. *Spectra properties*

The IR spectrum provides further evidence for the structure of the complex. The strong broad bands in the range $3440 \sim 3376\,\mathrm{cm}^{-1}$ are attributed to the –O–H stretching vibrations of water, and the bands in the range of $3267 \sim 3114\,\mathrm{cm}^{-1}$ can be attributed to stretching of the coordinated –NH_2 group. The absence of

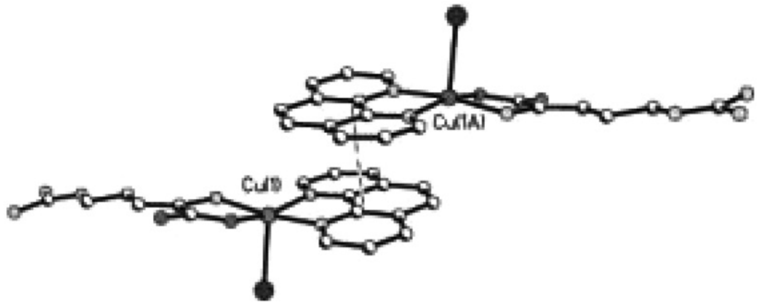

Figure 3. Intermolecular aromatic-stacking interaction of complex [Cu(phen)(*L*-arg)Cl]$_2 \cdot 7H_2O$ Symmetry transformations used to generate equivalent atoms: $-x$, $-y$, $1 - z$.

Table 3. Hydrogen bonds lengths (Å) for the title complex.

N(6) $\cdots$ O(8)	3.076(10)	N(6) $\cdots$ Cl(1)	3.358(8)
N(7) $\cdots$ O(7)	2.887(11)	N(10) $\cdots$ Cl(1)	3.219 (8)
N(8) $\cdots$ O(10)	2.907(13)	O(6) $\cdots$ O(11)	3.230(13)
N(9) $\cdots$ O(9)#1	2.855(11)	N(2) $\cdots$ O(7)	3.021(12)
N(10) $\cdots$ O(4)#1	3.013(12)	O(8) $\cdots$ O(5)	3.180(8)
N(11) $\cdots$ O(2)#2	2.891(11)	O(9) $\cdots$ O(10)#3	3.016(14)
N(5) $\cdots$ O(6)#3	2.891(11)	O(5) $\cdots$ N(12)	3.370(10)

Symmetry transformations used to generate equivalent atoms: #1: $x - 1$, y, z; #2: $x + 1$, y, z; #3: $1 - x, 1 - y$, $1 - z$.

any band in the region $1750 \sim 1700\,\mathrm{cm}^{-1}$ in the IR spectra of the isolated complex suggests coordination of the –COO$^-$ group of *L*-arginate to copper(II). Bands in the range of $1650 \sim 1635\,\mathrm{cm}^{-1}$ and $1394 \sim 1384\,\mathrm{cm}^{-1}$ can be attributed, respectively, to the antisymmetric and symmetric stretching vibrations of the coordinated carboxylate, with $\Delta v_{-\mathrm{co2}}$ values ($v^{as}_{-\mathrm{co2}} - v^{s}_{-\mathrm{co2}} > 200\mathrm{cm}^{-1}$) consistent with monodentate coordination [31–34]. Thus, one can deduce that *L*-arginate coordinates to copper(II) as bidentate *N*,O-ligands, confirmed by the result obtained by *X*-ray diffraction. Bands at $1575\,\mathrm{cm}^{-1}$, from the stretching vibration of the C=N group of phen, is weaker than that of free phen and the $\delta_{\mathrm{C-H}}$ (854, $740\,\mathrm{cm}^{-1}$) of phen shift to 851 and $724\,\mathrm{cm}^{-1}$, confirming coordination of phen nitrogen atoms to Cu(II).

The electronic spectrum in water presents four important absorption bands. The bands at about 203, 223 and 274 nm, are due to intra-ligand π ã π^* transitions of the phen-rings, showing two nitrogen atoms bonded to copper(II). The peak at 613nm of the complex is the d → d* transitions of copper(II) ions [31–35].

3.3. *SOD-like activity*

Under illumination, riboflavin (V_{B2}) reacts with tetramethylethylenediamine [$(CH_3)_2N(CH_2)_2N(CH_3)_2$] producing superoxide radical anion $\left(O_2^{\cdot -}\right)$:

$$V_{B2} + (CH_3)_2N(CH_2)_2N(CH_3)_2 \rightarrow O_2^{\cdot -} \qquad (1)$$

Nitro blue tetrazolium (NBT) reacts with $O_2^{\cdot -}$; but complexes or native CuZn–SOD will also:

$$\mathrm{NBT} + O_2^{\cdot -} \rightarrow \text{blue formazane (royal purple)} \qquad (2)$$

$$\text{Complexes or native CuZn} - \text{SOD} + O_2^{\cdot -} \rightarrow \mathrm{P} \qquad (3)$$

Blue formazane may be monitored at 560 nm by spectrophotometer. Complex or native CuZn–SOD react with $O_2^{\cdot -}$ by competing with NBT (equation (3)) after they are added to the blank solution, and formation rates of blue formazane would decrease. Relationships between the absorbence values of the solutions (absence and presence of the complex or native CuZn–SOD in blank solution) and different times are shown in figure 4. The slope of line shows the rate of NBT reduction by $O_2^{\cdot -}$ (equation (2)). Smaller slope values of the lines are correspond to larger concentrations of the complex or native CuZn–SOD in blank solutions (figure 4), indicating larger inhibition of NBT reduction by complex or native CuZn–SOD. One can conclude that the rate of $O_2^{\cdot -}$ decaying becomes faster with increasing concentrations of the complex or native CuZn–SOD. We can get the percentage inhibition (η) of NBT reduction by the complex or native CuZn–SOD according to the formula: $\eta = (1 - k'/k) \times 100\%$, where k' and k are slope values of lines in the presence and absence of the complex or native CuZn–SOD in blank solution, respectively, and then can obtain relationships between inhibition (η) and concentration (c) of the complex (figure 5). According to the formula $K_Q = K_N \cdots c(\mathrm{NBT})(k/k' - 1)/c(\mathrm{Q})$, we can get the rate constants K_Q of the catalyzed

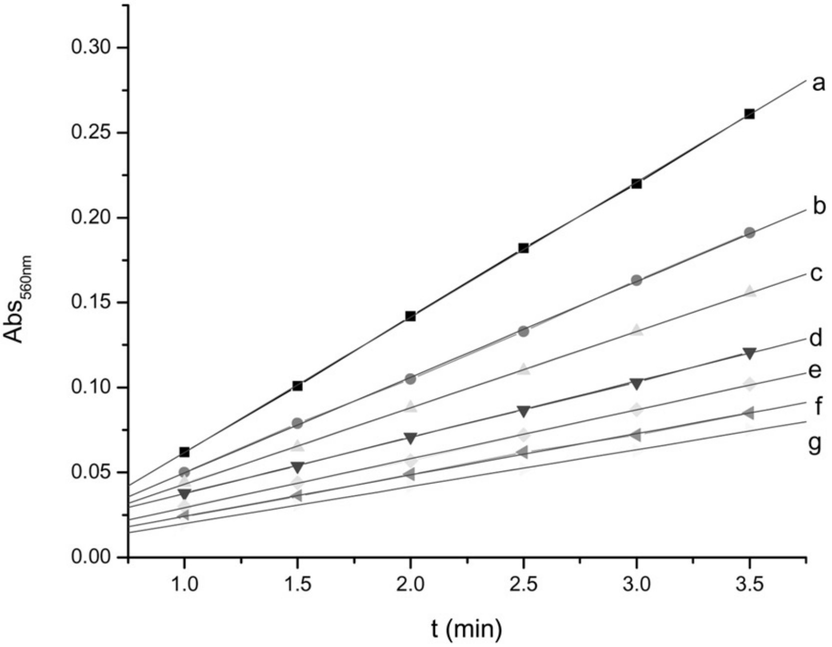

Figure 4. Absorbency values of various concentrations of $[Cu(phen)(L\text{-arg})Cl]_2 \cdot 7H_2O$ in solutions 25 pH 7.8; a: blank solution; b: $0.05\,\mu mol\,dm^{-3}$; c: $0.1\,\mu mol\,dm^{-3}$; d: $0.2\,\mu mol\,dm^{-3}$; e: $0.4\,\mu mol\,dm^{-3}$; f: $0.6\,\mu mol\,dm^{-3}$; g: $0.8\,\mu mol\,dm^{-3}$.

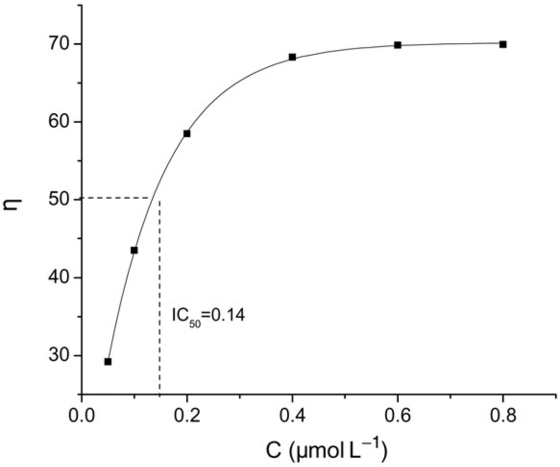

Figure 5. Relationship between the inhibition rate and concentration of the complex $[Cu(phen)(L\text{-arg})Cl]_2 \cdot 7H_2O$.

reaction of the complex and native CuZnSOD, where $K_N = 6.0 \times 10^4\,mol^{-1}\,dm^3\,s^{-1}$, c(NBT) and c(Q) represent the concentrations of nitro blue tetrazolium and the complex or native CuZn–SOD, respectively.

The IC_{50} and K_Q values of the complex, similar complexes in the literature [19–21] and native CuZn–SOD are listed in table 4. The activity of native CuZn–SOD determined this study is approximately that reported by Bonomo *et al.* [36], indicating the NBT

Table 4. IC_{50} and K_Q values of the complex and native CuZn–SOD for disproportionation of $O_2^{\cdot-}$.

Complex	IC_{50}^a (μmol dm^{-3})	K_Q (mol^{-1} dm^3 s^{-1})	Reference
Native CuZnSOD	0.0147	3.82×10^8	This work
$[Cu(phen)(L\text{-arg})Cl]_2 \cdot 7H_2O$	0.14	5.19×10^7	This work
$[Cu(phen)(L\text{-val})(H_2O)]Cl \cdot H_2O$	0.248	4.96×10^7	[19]
$[Cu(phen)(L\text{-ala})(H_2O)]Cl \cdot 4H_2O$	0.147	5.65×10^7	[20]
$[Cu(phen)(L\text{-gln})(H_2O)]Cl \cdot 2H_2O$	0.381	1.58×10^7	[20]
$[Cu(TATP)(L\text{-met})(H_2O)]NO_3 \cdot 0.5H_2O$	0.185		[21]
$Cu(amino\ acid)_2$	0.300 ~ 6.00		[42]
$CuCl_2$	0.27		This work

IC_{50} is the concentration for 50% inhibition of NBT reduction *L*-val = *L*-valine; *L*-ala = *L*-alaine; *L*-gln = *L*-glutamine; TATP = 1,4,8,9-tetraazatriphenylene; *L*-met = *L*-methionine.

method is credible. Phen and *L*-arg have no SOD-like activity, while $CuCl_2$ possesses SOD-like activity in the control experiment. Though the IC_{50} value of $CuCl_2$ is about two times that of the title complex, the presence of free Cu^{2+} has less influences on the SOD-like activity of the title complex.

The IC_{50} value of the title complex close to those of similar complexes [19–21] showing high SOD-like activity in solution. Furthermore, these complexes have low weights and simple ligands, and their structures are similar to that of copper(II) ions in the native CuZn–SOD. Thus the structure/activity relationship is consistent with the former conclusion that the copper(II) complex with distorted square pyramidal geometry, whose axial position is occupied by weakly coordinated small ions will exhibit distinct SOD-like activity in solution [37, 38, 39]. The relatively high SOD activity of the title complex may be ascribed to easy dissociation of the weakly coordinated axial Cl^- to provide a site on copper(II) for $O_2^{\cdot-}$ bonding and facilitates geometrical changes induced by $O_2^{\cdot-}$ bonding [40, 41].

Supplementary data

The supplementary material has been sent to the Cambridge Crystallographic Data Centre, 12 Union Road, Cambridge CB21EZ, UK as supplementary material No. 645352 and can be obtained by contacting the CCDC. (Fax: t44-1223-336-033; Email: deposit@ccdc.cam.ac.uk; orhttp://www.ccdc.cam.ac.uk).

Acknowledgement

This work was supported by the Principal Foundation of South China Agricultural University, P.R. China (No. 2005X008).

References

[1] J.M. Leiro, E. Alvarez, J.A. Arranz, I.G.L. Siso, F. Orallo. *Biochem. Pharmacol.*, **65**, 1361 (2003).
[2] J.M. McCord, M.A. Edeas. *Biomed. Pharmacother.*, **59**, 139 (2005).

[3] M. Jurczuk, M.M. Brzóska, J. Moniuszko-Jakoniuk, M. Galażyn-Sidorczuk, E. Kulikowska-Karpińska. *Food Chem. Toxicol.*, **42**, 429 (2004).
[4] B. Zegura, T.T. Lah, M. Filipic. *Toxicology*, **200**, 59 (2004).
[5] V. Valls, C. Peiro, P. Muňiz, G.T. Saez. *Process Biochem.*, **40**, 903 (2005).
[6] S. Rinalducci, J.Z. Pedersen, L. Zolla. *Biochim. Biophys. Acta*, **1608**, 63 (2004).
[7] S.S. Leonard, G.K. Harris, X. Shi. *Free Radic. Biol. Med.*, **37**, 1921 (2004).
[8] O. Vajragupta, P. Boonchoong, H. Watanabe, M. Tohda, N. Kummasud, Y. Sumanont. *Free Radic. Biol. Med.*, **35**, 1632 (2003).
[9] O. Vajragupta, P. Boonchoong, Y. Sumanont, H. Watanabe, Y. Wongkrajanga, N. Kammasuda. *Bioorg. Med. Chem.*, **11**, 2329 (2003).
[10] G.N. Landis, J. Tower. *Mech. Ag. Develop.*, **126**, 365 (2005).
[11] V.L. Kinnula, J.D. Crapo. *Free Radic. Biol. Med.*, **36**, 718 (2004).
[12] D.S. Clair, Y.F. Zhao, L. Chaiswing, T. Oberley. *Biomed. Pharmacother.*, **59**, 209 (2005).
[13] F.Z. Wang, Q.B. Wang, S.Y. Kwon, S.S. Kwak, W.A. Su. *J. Plant Physiol.*, **162**, 465 (2005).
[14] D.S. Selote, S. Bharti, R. Khanna-Chopra. *Biochem. Biophys. Res. Commun.*, **314**, 724 (2004).
[15] X. Bo, J.X. Li. *J. Beijing Union University (Natural Sciences)*, **20**, 17 (2006).
[16] S.V. Joan. *J. Chem. Edu.*, **62**, 990 (1985).
[17] J. Casanova, G. Alzuet, S. Ferrer, J. Latorre, J.A. Ramírez, J. Borrás. *Inorg. Chim. Acta*, **304**, 170 (2000).
[18] R. Pogni, M.C. Baratto, E. Busi, R. Basosi. *J. Inorg. Biochem.*, **73**, 157 (1999).
[19] X.Y. Le, S.R. Liao, X.P. Liu, X.L. Feng. *J. Coord. Chem.*, **59**, 985 (2006).
[20] X.Y. Le, S.R. Liao, Q.B. Lin, Q.M. Lu, X.P. Liu, Y.H. Xiong, X.L. Feng. *Chinese J. Inorg. Chem.*, **22**, 201 (2006).
[21] Q. Gu, S.R. Liao, Q.M. Lu, X.P. Liu, X.Y. Le. *Chem. Reas. Appl.*, **18**, 76 (2006).
[22] A.E.O. Fisher, D.P. Naughton. *Biomed. Pharmacother.*, **59**, 158 (2005).
[23] R. Pogni, M.C. Baratto, E. Busi, R. Basosi. *J. Inorg. Biochem.*, **73**, 157 (1999).
[24] Brucker AXS, *SAINT+ Version, 6.0* Brucker AXS, Madision, WI, USA (1999).
[25] R. Blessing. *Acta Crystallo.*, **A55**, 33 (1995).
[26] A. J. Wilson, *International Tables for X-ray Crystallography*, Kluwer Academic Publishers, Dordrecht, 1992, Tables p. 500, p. 219.
[27] G.M. Sheldrick, *SHELXS-97, Program for X-ray Crystal Structure Determination*, Göttingen University, Germany (1997).
[28] G. M. Sheldrick, *SHELXL-97, Program for X-ray Crystal Structure Refinement*, Göttingen University, Germany (1997).
[29] Z.R. Liao, X.F. Zheng, B.S. Luo, L.R. Shen, D.F. Li, H.L. Liu, W. Zhao. *Polyhedron*, **20**, 2813 (2001).
[30] W.J. Gear. *Coord. Chem. Rev.*, **7**, 81 (1971).
[31] X.H. Zhou, X.Y. Le. *Chemical Research in Chinese Universities*, **21**, 119 (2005).
[32] X.H. Zhou, C. Yang, X.Y. Le, S. Chen. *J. Coord. Chem.*, **57**, 401 (2004).
[33] X.Y. Le, M.L. Tong. *Chinese J. Inorg. Chem.*, **18**, 1023 (2002).
[34] X.H. Zhou, X.Y. Le, S. Chen. *J. Coord. Chem.*, **58**, 993 (2005).
[35] T. Sugimori, H. Masuda, N. Ohata, K. Koiwai, A. Odani, O. Yamauchi. *Inorg. Chem.*, **36**, 576 (1997).
[36] R.P. Bonomo, V. Bruno, E. Conte, G.D. Guidi, D.L. Mendola, G. MacCarrone, F. Nicoletti, E. Rizzarelli, S. Sortinoa, G. Vecchioa. *Dalton Trans.*, **23**, 4406 (2003).
[37] Z.N. Chen, Z.W. Mao, W.X. Tang. *Chemical Chin. Chem. Lett.*, **6**, 1 (1993).
[38] D. Chen, Q.W. Hang, Z.J. Liu, W.X. Tang, A.B. Dai. *J. Inorg. Chem*, **18**, 17 (1992).
[39] Z.R. Liao, H.H. Fu, T.L. Tian, H.L. Cai, W.Q. Liu. *Prog. Biochem. Biophys.*, **23**, 159 (1996).
[40] A.L. Abuhijleh, C. Woods. *Inorg. Chem. Commun.*, **5**, 269 (2002).
[41] K. Jitsukawa, M. Harata, H. Arii, H. Sakurai, H. Masuda. *Inorganica Chimica Acta*, **324**, 108 (2001).
[42] D.Z. Li, Z.M. Chen, Q. Jin. *J. Beijing Normal University (Nature Science)*, **32**, 251 (1996).